

Initial Study on Pulse Wave Velocity Acquired from One Hand Using Two Synchronized Wireless Reflectance Pulse Oximeters

Kejia Li, *Student Member, IEEE* and Steve Warren, *Member, IEEE*

Abstract—Pulse wave velocity (PWV) has garnered attention as a means to estimate vessel elasticity. This paper presents an approach to measure PWV using two synchronized, wireless pulse oximeters placed on the wrist and fingertip of the same hand. A MATLAB interface acquires and time-aligns these incoming photoplethysmograms (PPGs), and then it calculates PWVs using time differences at three waveform features: the foot, inflection point, and peak of the rising slope in each PPG. Consistent with expectations, PWV values for inflection points are larger than those calculated at waveform feet, since PWV is known to increase with increased intra-arterial pressure. However, the presence of pulse wave reflections complicates the interpretation of PWVs calculated from the PPG peaks since the reflected components impose a varying time delay on the related peaks.

Keywords—photoplethysmogram, pulse oximetry, pulse wave velocity

I. INTRODUCTION

PULSE oximetry estimates arterial oxygen saturation using baseline-normalized photoplethysmograms (PPGs) acquired with several wavelengths of excitation light [1]. The periodicity in these pulsatile waveforms is intuitively related to heart rate since arterial blood volume and flow (and therefore optical absorption due to hemoglobin) track the cardiac cycle. Related research notes that physiologic parameters such as blood pressure, respiration rate, and stroke volume can also be derived from PPGs [2], [3].

Pulse wave velocity (PWV) has attracted attention as an arterial elasticity indicator. PWV methods that utilize PPGs include 1) pulse transit time (PTT) extracted from time-correlated ECGs and PPGs [4], 2) transit time acquired from dual-channel (finger and toe) PPGs [5], and 3) peak-to-peak time (PPT) from a single digital volume pulse (DVP) waveform [6] (also tested in our early efforts [7], [8]). Other PWV estimation modalities include ultrasonic Doppler [9].

A direct way to calculate average wave velocity is the distance between two locations divided by the wave transit time. Obstacles for using this method to calculate PWV with PPGs include 1) at least one of the two locations on the same arterial segment makes PPG acquisition difficult with a

transmittance-mode sensor (e.g., one sensor on the fingertip and the other at the wrist), 2) PWV is much faster than blood flow, requiring a pulse oximeter to sample at a high rate to ascertain the transit time for a PPG waveform acquired at two locations separated by a short distance, 3) the two pulse oximeters or PPG acquisition devices must be synchronized, and 4) the PPG signal must be high quality (e.g., thousands of digitization levels, high signal-to-noise ratio, and undistorted), especially when considering that PWV varies as vessel walls dilate and constrict during each heart cycle.

This paper presents an initial study on PWV estimation using a pair of low-cost, custom wireless reflectance pulse oximeters at two measurement locations on the same hand. While larger scale tests are pending and the results are not verified against commercial medical equipment, this short investigation offers insight into the design issues related to an economical single-hand approach, including changes to downstream versus upstream signal shape caused by intra-cycle changes in arterial pressure.

II. THEORY

PWV can be expressed as a function of arterial elasticity via the Moens-Korteweg equation [10]:

$$PWV = \sqrt{\frac{hE_{inc}}{2r\rho}} \quad (1)$$

where h is the arterial wall thickness, E_{inc} is the incremental elastic modulus, r is the lumen radius, and ρ is the blood density. When PWV is measured with one of the aforesaid methods, arterial parameters such as arterial elasticity could be estimated by the reverse solution of (1). For instance, a high relative PWV in the aorta may suggest a stiffer arterial wall in some individuals. As implied in *Section I. Introduction*, PWV is not constant even in the same vessel segment. Rather, it can be derived as a monotonically increasing function of pressure. I.e., PWV is different when measured at different stages of the cardiac cycle [10].

III. METHODS

A. Study Description and Experimental Setup

Custom wireless reflectance pulse oximeters were employed to simultaneously acquire PPGs from the wrist and fingertip (middle finger). Each pulse oximeter yields four PPG channels: separate pulsatile (AC) and baseline (DC) sample sequences for the red and near-infrared excitation wavelengths. The sampling frequency is $f_s = 240$

Manuscript received March 26, 2011; accepted June 8, 2011. This work was supported in part by the National Science Foundation under grants BES-0093916, CNS-0932289, and CNS-0551626. Opinions, findings, conclusions, or recommendations expressed in this material are those of the author(s) and do not necessarily reflect the views of the NSF.

Kejia Li and Steve Warren are with the Department of Electrical & Computer Engineering, Kansas State University, Manhattan, KS 66506, USA (kejiali@ksu.edu; swarren@ksu.edu).

Hz to avoid aliasing, e.g., 120 Hz flicker from full-wave-rectified fluorescent room lights. Each channel is unfiltered and has a precision of 4096 digitization levels that correspond to a (0, 2.4) V range.

Since 1) blood oxygen saturation is not the focus of this effort and 2) each near-infrared channel exhibits better signal quality than its red counterpart, only the near-infrared AC and DC channels of the two devices are utilized for PWV calculations. The DC signal (also referred to as the ‘baseline’ in this paper) is not a constant in this model. It is controllable and may jump (change value instantly) to resist saturation of AC signal; the influence of the jump on the AC signal is removed later. More details are described in [7].

When synchronized PPG waveforms from two pulse oximeters placed at the wrist and the fingertip (see Fig. 1) are ready, time differences can be extracted from point pairs on the corresponding curves. A typical PPG cycle has a steep rising slope and a mild falling slope consistent with the systolic and diastolic durations in the cardiac cycle. For this study, three point pairs were selected at different waveform features: 1) the valley (foot), 2) the inflection point on the rising slope and 3) the time corresponding to the rising-slope peak. This offers the opportunity to calculate and compare three PWV values at different intra-arterial pressure levels. In other words, this work was initiated to see whether the estimated PWVs are consistent with PWVs obtained using other methods, such as PPT from DVP, and whether PWV exhibits measurable dependency on pressure.

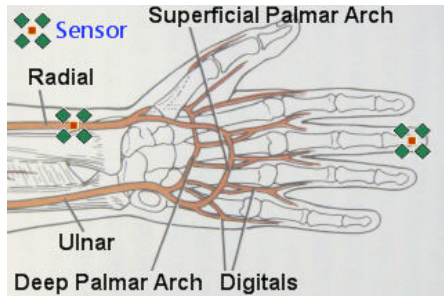


Fig. 1. Measurement setup with one pulse oximeter (sensor) at the wrist and the other at the fingertip. The primary arterial tree of the hand is depicted to illustrate the pulse travel path. This figure is adapted from [11].

B. Signal Synchronization

A MATLAB interface (Fig. 2) collected, through serial communication, near-infrared data acquired by two pulse oximeters. The respective communication parameters (serial port, sample rate, signal channel, wireless channel, and refresh rate) can be set on the left panel. Note that the displayed near-infrared waveforms in the two sub-windows on the right are visualized in a ‘first ready, first displayed’ unsynchronized manner. However, the PPG signals generated by the two pulse oximeters must be synchronized so as to accurately extract the relative time delay on the waveform acquired from the distal sensor, where the sensor-to-sensor distance is known. Hence, an interface feature was developed that ‘punches’ the data sets when they are dumped from two separate serial buffers at the same time. This ‘punch’ method ensures that the punched points on the

two waveforms are time synchronized.

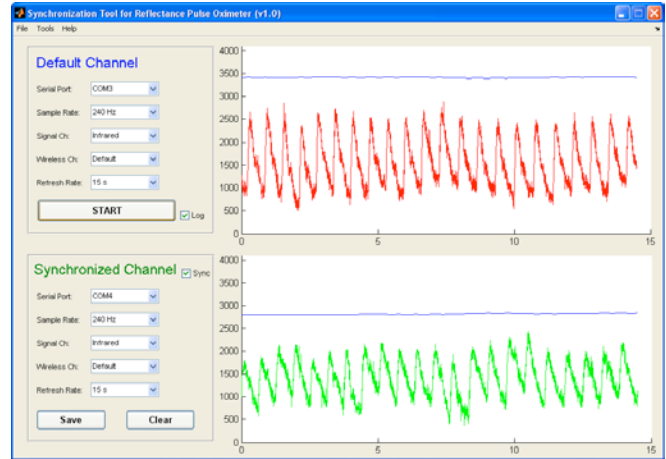


Fig. 2. A MATLAB interface that simultaneously communicates with two pulse oximeters on different serial ports.

Fig. 3 illustrates two PPG waveforms that are synchronized by aligning the corresponding punched points in their data sets. The punch dots on these AC channels have a uniform value of 2048. The DC/baseline channels are also punched (not shown here) to further confirm the punch dots.

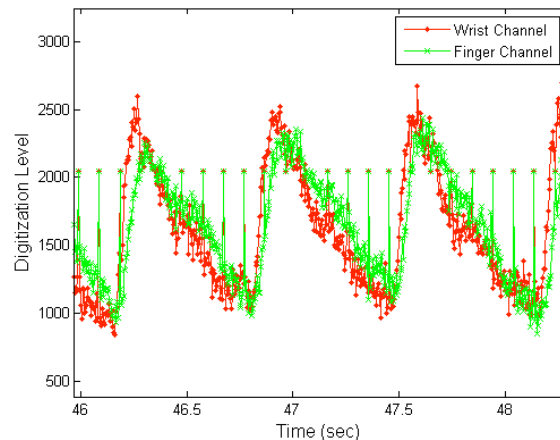


Fig. 3. Punched raw PPG waveforms that are aligned (synchronized).

C. Signal Preprocessing

Removing the punched points from the synchronized signals yields raw PPGs (see Fig. 4) for further processing. The second preprocessing step is to filter the raw PPGs. The filter is a 240th-order lowpass filter with a 5 Hz cutoff frequency realized with a MATLAB function `firls()`, a linear-phase FIR filter that uses least-squares error minimization. This high-order filter causes a time delay of $t_d = (n-1)/(2f_s) = 0.498$ seconds, where $n = 240$ and $f_s = 240$ Hz. The group time delay equally pushes all cycles (including each of their individual frequency components) to the right as seen in Fig. 5 when compared to Fig. 4 without phase distortion. The cutoff frequency is set to the relatively low value of 5 Hz to ensure smooth derivative curves (see Fig. 6). A higher cutoff frequency would require a method such as curve fitting to be employed when extracting the associated delays from these derivative data.

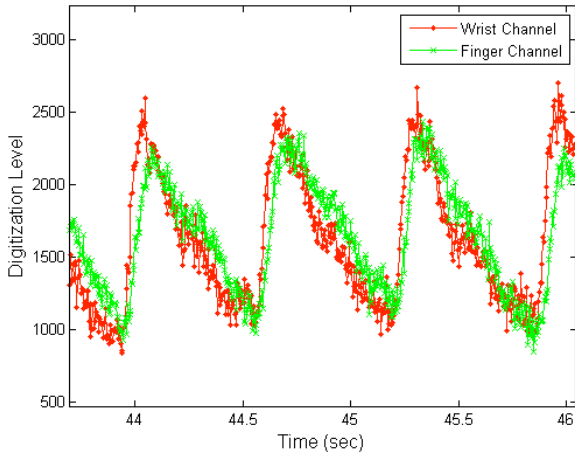


Fig. 4. Synchronized raw PPG waveforms with the punch marks removed.

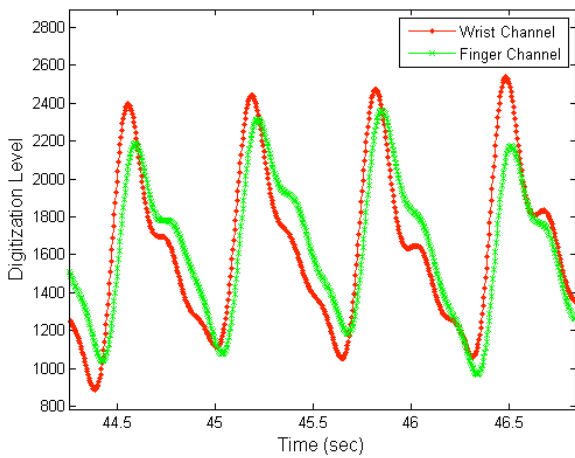


Fig. 5. Filtered PPG waveforms. The channels are still synchronized due to the same group delay imposed by the linear-phase lowpass filter.

D. Pulse Travel Time Extraction

The time difference between the two PPG waveforms becomes clearer after filtering. Because of the discrete signal nature, the time axis is really a count axis. Fig. 6(a) depicts this idea with a pair of filtered, single-cycle PPGs, each containing ~ 150 data points. The time duration between consecutive samples is $1/f_s = \sim 0.417$ milliseconds, the best time resolution available. To identify the corresponding PPG feet and peak locations, the first derivative was employed (see Fig. 6(b)). The second derivative was used to locate inflection points on the rising slope (see Fig. 6(c)). Count delays were subsequently extracted using the zero values of the appropriate differentiated data, as illustrated in Fig. 6.

IV. RESULTS AND DISCUSSION

A. Count Differences

A ten-second pair of near-infrared PPG segments was chosen, where the selection criterion was minimal variation in the baseline, which is preferred since severe baseline fluctuations normally imply motion. Each segment contains 2400 ($10 f_s$) data points and 15 whole PPG cycles (rising slopes), which means that 15 sets of time differences/PWVs

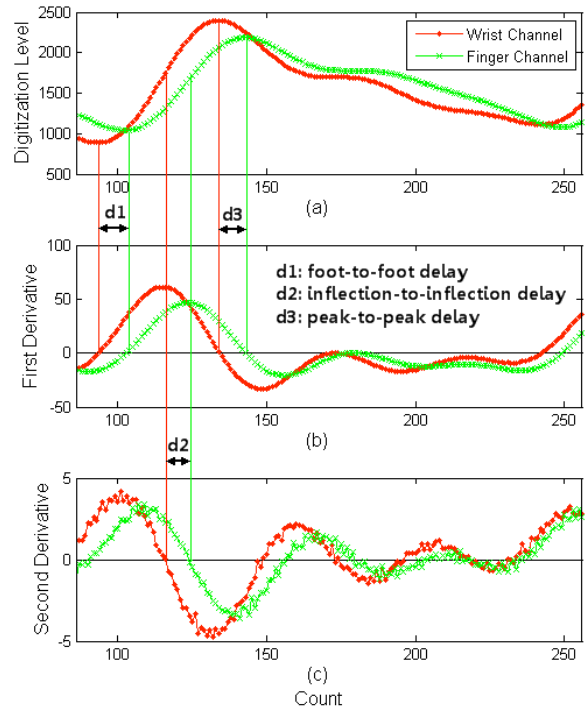


Fig. 6. First derivative (b) and second derivative (c) of a pair of filtered single-cycle PPGs (a). Three delays, d1, d2, and d3, are extracted according to the count differences represented by the line at $y = 0$ in (b) and (c).

can be extracted and averaged for each waveform feature. The results are detailed in Table 1. Taking the first cycle as an example, as in Fig. 6, the foot indices for the wrist and fingertip PPGs are 94 and 103, respectively, so the FTF (foot-to-foot) delay is $103 - 94 = 9$ counts. Likewise, the ITI (inflection-to-inflection) delay is $124 - 116 = 8$ counts, and the PTP (peak-to-peak) delay is $143 - 134 = 9$ counts.

Averaging these values over 15 cycles yields $FTF = 7.1$ counts, $ITI = 6.5$ counts, and $PTP = 8.3$ counts. The corresponding standard deviations are as high as 1.5 counts, which is relatively large. Though the pulse oximeter has a 240 Hz sampling rate, only 6-to-8 counts exist between similar features on the two waves: PWV is much faster than blood flow. Considering that the red channel does not contribute to PWV calculation, we assume that the removal of those code blocks from the firmware could improve the sampling frequency to 480 Hz.

B. Pulse Wave Velocity Estimation

Count differences can be converted into time differences in seconds by dividing by f_s . If the pulse travel length (TL in Table I) between the sensors is measured, the three variations on PWV can be calculated from the time differences. The distance between two measurement locations is 0.224 m; however, the arterial distance is slightly longer when one considers the indirect paths in the arterial tree of the hand (see Fig. 1.). A subjective factor of 1.25 was therefore used to get $TL = 0.224 * 1.25 = 0.280$ m. The PWVs using this estimated TL are listed in Table I.

As noted in Section II. Theory, PWV should increase as pressure increases, which occurs along the rising slope of a

TABLE I
PWV RESULTS FROM A TEN-SECOND PPG WAVEFORM PAIR FROM ONE SUBJECT

Cycle	Wrist Foot	Finger Foot	Wrist Peak	Finger Peak	Wrist Inflect.	Finger Inflect.	FTF (count)	ITI (count)	PTP (count)	TL (m)	FTF (m/s)	ITI (m/s)	PTP (m/s)
1	94	103	134	143	116	124	9	8	9	0.280	7.47	8.40	7.47
2	242	249	286	293	266	272	7	6	7		9.60	11.20	9.60
3	396	403	437	445	419	425	7	6	8		9.60	11.20	8.40
4	556	562	596	603	579	584	6	5	7		11.20	13.44	9.60
5	711	719	752	760	734	740	8	6	8		8.40	11.20	8.40
6	870	877	910	918	892	898	7	6	8		9.60	11.20	8.40
7	1037	1045	1077	1087	1059	1067	8	8	10		8.40	8.40	6.72
8	1205	1211	1244	1250	1226	1232	6	6	6		11.20	11.20	11.20
9	1365	1370	1406	1415	1388	1392	5	4	9		13.44	16.80	7.47
10	1527	1533	1566	1576	1548	1555	6	7	10		11.20	9.60	6.72
11	1690	1698	1731	1740	1712	1719	8	7	9		8.40	9.60	7.47
12	1847	1855	1888	1896	1870	1875	8	5	8		8.40	13.44	8.40
13	2000	2009	2042	2052	2024	2032	9	8	10		7.47	8.40	6.72
14	2156	2160	2197	2204	2178	2185	4	7	7		16.80	9.60	9.60
15	2311	2320	2353	2362	2334	2342	9	8	9		7.47	8.40	7.47
AVG = Average							AVG	7.13	6.47	8.33	9.91	10.80	8.24
STD = Standard Deviation							STD	1.50	1.24	1.23	2.57	2.36	1.30

FTF = foot-to-foot; ITI = inflection point to inflection point; PTP = peak-to-peak. TL = travel length of pulse wave at the hand.

PPG. Hence, PWVs calculated from the feet, inflection points, and peaks of the rising slopes should be ordered from least to greatest. These early results do indicate an increase in average PWV from the foot (9.9 m/s) to the inflection point (10.8 m/s) but a decrease at the peak (8.2 m/s). The next two paragraphs contain thoughts in that regard.

First, a PPG as in Fig. 6 is composed of two waveforms that correspond to different time delays: 1) the systolic (or direct) component that results from the direct transmission of the systolic pressure wave from the aorta to the arm and 2) the diastolic (or reflected) component that results from the reflection of the pressure wave from the peripheral arteries to the aorta and then back to the arm [8], [10]. The peak of the rising slope therefore experiences dispersion caused by these wave reflections, which also result in minor peaks that appear on the falling PPG slope. Effects of reflections on PWV values are also noted in [10].

Second, two small arteries converge in the fingertip: one from the superficial palmar arch and the other from the deep palmar arch. These arches bridge the radial artery (where the other device is placed) and the ulnar artery. This structure makes the fingertip pulse waveform more complex than the waveform one would model for a simple vessel segment.

V. CONCLUSION

This paper presented a method to determine PWV in the hand using two reflectance-mode, wireless pulse oximeters placed at the wrist and fingertip. PWV values obtained at different features of the corresponding PPGs (foot, inflection point, and rising-slope peak) support the assertion that PWV depends on arterial pressure. PPG foot and inflection-point calculations show an increase in PWV as arterial pressure increases, but peak-based calculations are inconsistent with expectations, primarily because the effects of wave reflections on PPG shape are not well modeled and warrant

further investigation. Nonetheless, the two-oximeter approach was shown to be feasible, so the next logical step is to compare these PWVs with values obtained from commercial devices employing other modalities.

REFERENCES

- [1] K. K. Tremper, "Pulse Oximetry," *Chest*, vol. 95, pp. 713-715, April 1989.
- [2] A. Reisner, P. A. Shaltis, D. McCombie, and H. H. Asada, "Utility of the Photoplethysmogram in Circulatory Monitoring," *Anesthesiology*, vol. 108, pp. 950-958, May 2008.
- [3] K. H. Shelley, "Photoplethysmography: Beyond the Calculation of Arterial Oxygen Saturation and Heart Rate," *Anesthesia & Analgesia*, vol. 105, pp. S31-S36, Dec. 2007.
- [4] J. Sol'a, O. Ch'etelat, C. Sartori, Y. Allemann, and S. F. Rimoldi, "Chest Pulse-Wave Velocity: A Novel Approach to Assess Arterial Stiffness," *IEEE Transactions on Biomedical Engineering*, vol. 58, Jan. 2011.
- [5] H.-T. Wu, C.-S. Ho, J.-S. Weng, W.-C. Tsai, and M.-C. Wang, "A Novel Method for Measurement of Pulse Wave Velocity by Dual-Channel Photoplethysmography," *2004 IEEE International Workshop on Biomedical Circuits & Systems*, 2004, pp. S2/6-8-10.
- [6] S. R. Alty, N. Angarita-Jaimes, S. C. Millasseau, and P. J. Chowienzyk, "Predicting Arterial Stiffness From the Digital Volume Pulse Waveform," *IEEE Transactions on Biomedical Engineering*, vol. 54, pp. 2268-2275, Dec. 2007.
- [7] K. Li and S. Warren, "A Wireless Reflectance Pulse Oximeter Suitable for Wearable and Surface-Integratable Designs That Produces Unfiltered Photoplethysmograms," *IEEE Transactions on Biomedical Circuits and Systems*, submitted for publication.
- [8] K. Li and S. Warren, "A High-Performance Wireless Reflectance Pulse Oximeter for Photo-Plethysmogram Acquisition and Analysis in the Classroom," *2010 Annual Conference and Exposition of the ASEE*, Louisville, KY, June 20-23, 2010.
- [9] N. Chubachit, H. Kanait, R. Muratat, and Y. Koiwa, "Measurement of Local Pulse Wave Velocity in Arteriosclerosis by Ultrasonic Doppler Method," *1994 IEEE Proceedings on Ultrasonics Symposium*, Cannes, France, Nov. 1-4, 1994, pp. 1747-1750.
- [10] N. Westerhof, N. Stergiopoulos, and M. I. M. Noble, *Snapshots of Hemodynamics*, 1st ed. Boston: Springer, 2004.
- [11] A. P. Spence, *Basic Human Anatomy*, 1st ed. Menlo Park: The Benjamin/Cummings Publishing Company, Inc., 1982.